A waveguide polarizer based on Si-coated Ti:$LiNbO_3$ planar structure

Hangyou Lin (林航友)[1], Jiping Ning (宁继平)[1], and Fan Geng (耿 凡)[2]

[1] *College of Precision Instrument and Opto-Electronics Engineering, Optoelectronic Information Science & Technology Lab, MOE, Tianjin University, Tianjin 300072*

[2] *The 8358th Institute, The Third Academy, CASA, Tianjin 300072*

Received September 11, 2003

A novel design of a transverse magnetic (TM)-pass waveguide polarizer based on Si on an X-cut, Y-propagation Ti:$LiNbO_3$ planar waveguide is presented. The eigenvalue functions of such structure have been obtained by using Wenzel-Kramers-Brillouin (WKB) method with modified Airy functions. The intervals of the silicon thickness have been found which result in transverse electric (TE) light suffering strong attenuation while TM wave propagating with fairly low loss. A planar waveguide polarizer is fabricated and its polarization-dependent measurements lead to the best polarization extinction ratio ~ 34 dB and the insertion loss < 0.4 dB.

OCIS codes: 130.0130, 130.1750, 130.3730.

A waveguide polarizer is usually used as an important component in a large integrated optical circuit when polarization-dependent performance is desired. Most design principles of them are based on either making one of the basic transverse electric (TE) or transverse magnetic (TM) modes be subjected to exclusive loss or employing interferometric concepts. Among various designs, overlays on waveguides are strongly absorbing metallic, highly refracting and birefringent transparent materials. So far, metal-clad Ti-indiffusion, proton-exchange and Zn-indiffusion are the three well-known methods of making single polarization waveguides on $LiNbO_3$[1−4]. Recently, Si overlays on lithium niobate waveguide structures have been proposed for many integrated optical devices[5−7]. On the one hand, silicon holds the promise for monolithic integration optical components on a single substrate, and it is the material of low-loss at the communications wavelength, of low cost, of large refractive index and easy to process. On the other hand, lithium niobate waveguides are used in many high performance passive and semi-active devices for their excellent elastooptical, electrooptical, piezoelectrical and pyroelectrical properties. Since a waveguige polarizer does not usually mean a device of its own, no need of extra materials and complicated processing steps are expected. Naturally, a polarizer based on Si-coated-$LiNbO_3$ waveguide structure comes into request. The ideal properties of large modulation of the effective mode index by Si overlays and low-loss Ti:$LiNbO_3$ waveguides will justify fabricating a high quality waveguide polarizer.

Figure 1 sketches the index profiles of the X-cut, Y-propagation Si-coated-Ti:$LiNbO_3$ planar waveguides structure. N, n_s and Δn denote effective mode index, substrate refractive index and surface index increment, respectively. Figures 1(a) and (b) correspond to the cases when $N \le n_s + \Delta n$ and $N \ge n_s + \Delta n$, respectively. n_0, n_f and n_s are the refractive indices of air-clad, Si film and substrate, respectively. The normalized displacement ζ and the normalized thickness of Si film ζ_f are defined as the ratio of x (the depth along the diffusion direction) and the silicon thickness to the effective Ti-indiffusion depth, i.e., $\zeta = x/d$ and $\zeta_f = d_{Si}/d$, respectively. ζ_t denotes the turning point. The profiles are truncated at a virtual interface ζ_s. Beyond ζ_s at the substrate side, the refractive-index is assumed to be equal to the substrate refractive-index n_s.

It is well known that both the electric and magnetic fields satisfy the one-dimensional Helmholtz equation

$$\left[\frac{d^2}{d\zeta^2} + \kappa^2\left(n^2(\zeta) - N^2\right)\right]\psi(\zeta) = 0, \tag{1}$$

where the scalar field ψ is proportional either to the y component of the TE field, i.e. $\psi \propto E_y$, or to the y component of the TM field, i.e. $\psi \propto H_y$. The normalized wave number κ is defined as the product of the vacuum wave number k_0 and d, i.e. $\kappa = k_0 d$. The refractive-index $n(\zeta)$ is given by the sum of the substrate index and local index increase[8]. By employing Wenzel-Kramers-Brillouin (WKB) method with modified Airy functions[9], the eigenvalue equation corresponding to Figs. 2(a) and (b) may take the forms as follows.

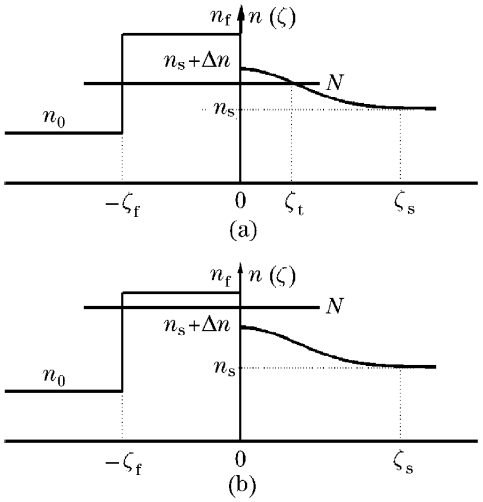

Fig. 1. Index profiles of the X-cut, Y-propagation Si-coated-Ti:$LiNbO_3$ planar waveguides structure.

Case A: $N \leq n_s + \Delta n$ as in Fig. 1(a)

$$\int_0^{\zeta_t} Q(\zeta)d\zeta = m\pi + \tan^{-1}\left[\sigma(0)\frac{\alpha_f}{Q(0^+)}\tan(\delta_f - \alpha_f\zeta_f)\right] + \frac{\pi}{4} + \tan^{-1}\left(\frac{1}{\sqrt{3}}\frac{1-h}{1+h}\right); \quad (2)$$

Case B: $N \geq n_s + \Delta n$ as in Fig. 1(b)

$$\alpha_f\zeta_f = m'\pi + \delta_f + \tan^{-1}\left(\frac{P(0^+)}{\sigma(0)\alpha_f}\right). \quad (3)$$

In Eqs. (2) and (3), m is the mode label in Ti-indiffusion waveguide, while m' denotes mode label of the whole waveguide structure; and with the abbreviations

$$\begin{cases} \alpha_0 = \kappa\sqrt{N^2 - n_0^2} \\ \alpha_f = \kappa\sqrt{n_f^2 - N^2} \\ Q(\zeta) = \kappa\sqrt{n^2(\zeta) - N^2} \\ P(\zeta) = \kappa\sqrt{N^2 - n^2(\zeta)} \end{cases}$$

$$\text{and} \begin{cases} \delta_f = \tan^{-1}\left(\frac{\alpha_0}{\alpha_f}\sigma(-\zeta_f)\right) \\ h = \frac{I_{2/3}(\varphi_s)+[1+1/(6\varphi_s)]I_{-1/3}(\varphi_s)}{I_{4/3}(\varphi_s)+[1+5/(6\varphi_s)]I_{1/3}(\varphi_s)}, \end{cases} \quad (4)$$

where $\sigma(\zeta) = n_0^2(\zeta^+)/n_0^2(\zeta^-)$ for TM case and $\sigma_0 = 1$ for TE case; and, $\varphi_s = \varphi(\zeta_s^-)$. $I_v(\cdot)$ is the modified Bessel function of the first kind.

The dependence of the refractive index of silicon on wavelength has been obtained by the curve-fitting in the form of Sellmeier Equation. The fitted curve and experimental data are shown in Fig. 2.

The effective mode indices against the thickness of Si film d_{Si} are obtained from Eqs. (2) and (3), and curves of these are plotted in Fig. 3. As can be drawn from this figure, periodic "forbidden regions" of Si thickness Δd are found. Within such interval, the mode index of the whole structure is between the surface indices of both polarizations, i.e., $n_{se} + \Delta n_e < N < n_{so} + \Delta n_o$. The TE light then suffers extreme attenuation while the TM wave does not. Naturally, if the thickness of Si film falls into one of such ranges, the structure will resemble a TE-mode waveguide isolator, and it is a TM-pass waveguide polarizer as well.

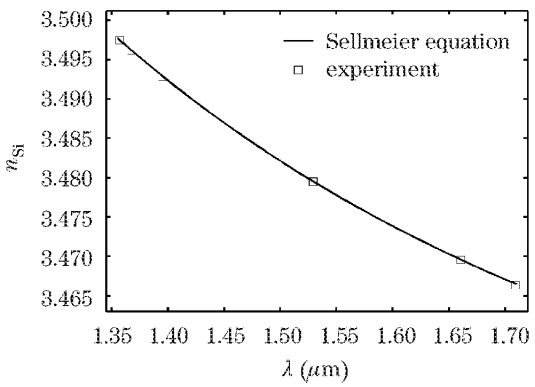

Fig. 2. The dependence of Si refractive-index on wavelength in the form of Sellmeier Equation. The relative experimental data is obtained from Ref. [10].

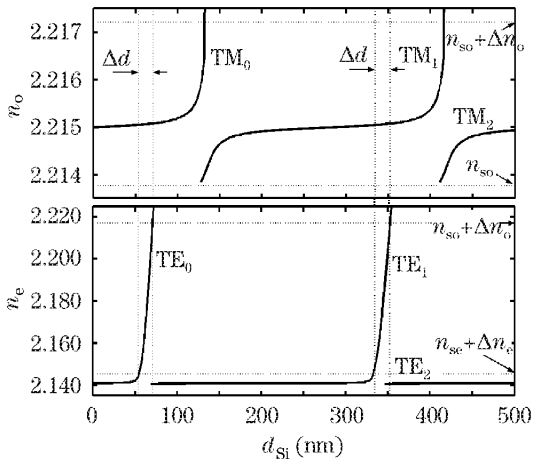

Fig. 3. Curves of the effective mode indices versus d_{Si} for a Si overlay on a Ti:$LiNbO_3$ waveguide supporting the fundamental modes of both polarizations corresponding the operation wavelength at 1.523 μm. The thickness of Ti-stripe is 32 nm and the diffusion duration is 9.5 hours at 1050 °C.

The vertical field profiles (along the x axis) are presented for $d_{Si} = 0.06$ and 1.00 μm in Fig. 4. As seen, the fields are almost completely confined in $LiNbO_3$ waveguide. Moreover, all curves corresponding to the different d_{Si} values resemble those of the TE_0 or TM_0 in the structure of no Si film with the exception of some lobes in Si overlays. (The field curve at $d_{Si} = 0$ is not plotted since it almost fully resembles that at $d_{Si} = 0.06$ μm.) Therefore, the structure holds the so-called "single-mode" behavior. At $d_{Si} = 0.06$ μm, the energy of TE_0 mode is essentially pulled away from $LiNbO_3$ waveguide, while TM_0 mode resides mainly in $LiNbO_3$ waveguide. Since the field curves are all corresponding to the excited modes at the input, the lobes are slightly high. If the longitudinal propagation absorption is under consideration, their magnitudes will be extremely low compared with the main lobe at the output, because these lobes are tightly confined in Si overlays and suffer considerable high-loss. For a TM selective polarizer, since very little

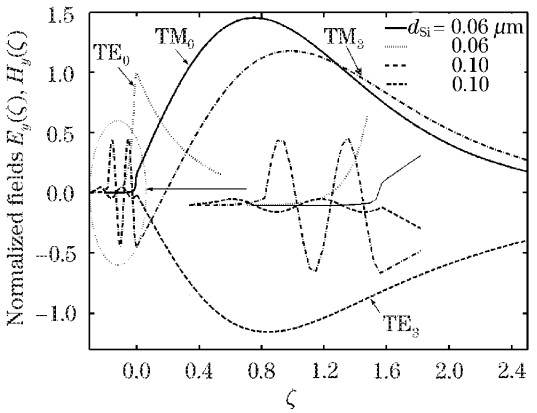

Fig. 4. Normalized vertical fields for $d_{Si} = 0.06$ and 1.0 μm. The TI waveguide parameters are the same as Fig. 4. The effective TI depth $d \approx 5.5$ μm. The imaginary part of Si refractive-index, $n_i \approx i0.002$[11], is under consideration. The change of n_i with respect to wavelength is neglected.

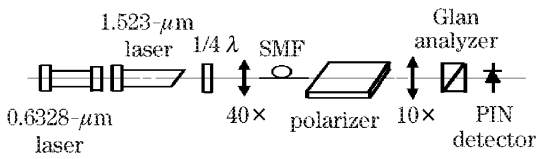

Fig. 5. Experimental setup.

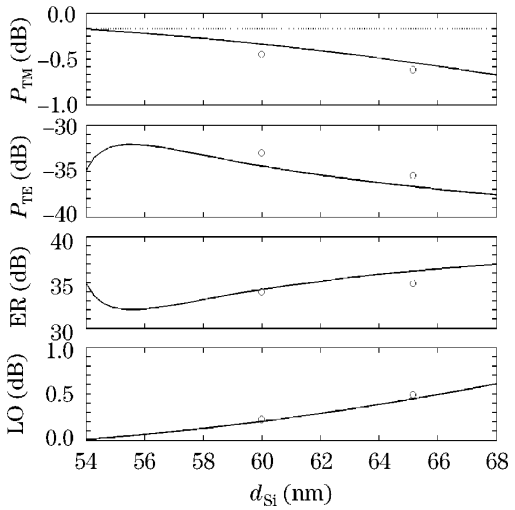

Fig. 6. Curves of TE and TM power transmissions P_{TE}, P_{TM}, extinction ratio ER, and insertion loss LO, versus the thickness of Si film d_{Si}. The solid lines are the theoretical results; circle markers are the experimental data, which correspond to the operation wavelength at 1.523 μm.

power of TM mode is carried in the lossy film, the net loss by Si overlay is fairly low. Hence, the insertion loss due to the existence of Si overlay is rather low in comparison with the coupling loss.

Two polarizers of Si on an X-cut, Y-propagation Ti:$LiNbO_3$ waveguides are fabricated. For one of them, the structural and fabrication parameters are $d_{Si} = 60$ nm, the thickness of Ti-stripe is 32 nm, diffusion duration 9.5 hours at 1050 °C and $L = 2$ mm (where L is the length of Si film along the longitudinal propagating direction), while for the other, the same parameters are chosen except $d_{Si} = 65$ nm.

We have measured the polarization extinction ratio of the polarizer using the experimental setup as shown in Fig. 5. The 0.6328-μm-wavelength laser light is employed to collimate the optical system and the 1.523-μm He-Ne laser is used as light source. A circular polarization light is obtained using the quarter-wave plate and coupled into the polarizer single mode fiber through a 40× lens. Then, the output light from the device is passed through a 10× lens and an analyzer and detected by a photodetector. Each polarization component of output light is measured by rotating the analyzer. The variations of the TE and TM power transmissions P_{TE}, P_{TM}, the extinction ratio ER, and the insertion loss LO as functions of d_{Si} are shown in Fig. 6. As seen, extinction ratio and insertion loss are dependent on the thickness of Si overlays. A polarizer with < 0.4 dB insertion loss and ~ 34 dB polarization extinction ratio is obtained.

In conlusion, the eigenvalue functions of Si-coated-Ti:$LiNbO_3$ structures have been obtained by using the WKB method with modified Airy functions. Periodic "forbidden zones" of Si thickness for TE-mode have been found. If Si thickness falls into this region, the structure will perform as a TE suppression waveguide polarizer. Such polarizer is a quite suitable component in Si-coated-$LiNbO_3$ integrated optical circuits.

This work was supported by the National Natural Science Foundation of China under Grant No. 10084001. H. Lin's e-mail address is hylin@vip.163.com.

References

1. O. Mikami, Appl. Phys. Lett. **36,** 491 (1980).
2. P. K. Wei and W. S. Wang, IEEE Photon. Technol. Lett. **6,** 245 (1994).
3. H. Maruyama, M. Haruna, and H. Nishihara, J. Lightwave Technol. **13,** 1550 (1995).
4. R.-C. Twu, C.-C. Huang, and W.-S. Wang, IEEE Photon. Technol. Lett. **12,** 161 (2000).
5. H. Robinson, C. W. Pitt, and R. A. Ginson, Appl. Opt. **32,** 3981 (1993).
6. C. P. Hussell and R. V. Ramaswamy, IEEE Photon. Technol. Lett. **9,** 636 (1997).
7. H. Feng, R. F. Tavlykaev, and R. V. Ramaswamy, Electron. Lett. **35,** 1636 (1999).
8. S. Fouchet, A. Carenco, C. Daguet, R. Guglielmi, and L. Riviere, J. Lightwave Technol. **5,** 700 (1987).
9. M.-S. Chung and C.-M. Kim, J. Lightwave Technol. **18,** 878 (2000).
10. http://www.crystran.co.uk/sidata.htm.
11. T. Conese, R. Tavlykaev, C. P. Hussell, and R. V. Ramaswamy, J. Lightwave Technol. **16,** 1113 (1998).